

# Microseismic evidence for horizontal hydraulic fractures in the Marcellus Shale, southeastern West Virginia



Abdulgader A. Alalli<sup>1</sup> and Mark D. Zoback<sup>1</sup>

## Abstract

An integrated analysis of multistage hydraulic fracture stimulation done in three horizontal wells in the Marcellus Shale in southeastern West Virginia revealed that nearly half (14 out of 31) of the examined stages initiated horizontal hydraulic fractures. The study was performed in an area characterized by a transitional strike-slip/reverse faulting stress state where the maximum horizontal principal stress ( $S_{Hmax}$ ) is oriented N55°E. The stages that produced horizontal hydraulic fractures were all within the organic-rich Lower Marcellus Shale. Two lines of evidence indicate horizontal hydraulic fracture propagation. The measured least principal stress of those stages was of similar magnitude to the vertical stress ( $S_v$ ), indicating that the vertical stress and microseismic events are limited to a narrow horizontal layer and do not propagate vertically out of the Lower Marcellus Shale. Both lines of argument indicate that the vertical stress is the least principal stress, perhaps due to viscoplastic stress relaxation in the clay- and kerogen-rich Lower Marcellus Shale. In the 17 stages where perforations were placed in the stiffer Onondaga and Cherry Valley formations, the measured least principal stresses were less than the magnitude of  $S_v$ , indicating that  $S_{hmin}$  was the least principal stress. The microseismic data indicate vertical hydraulic fracture propagation, principally upward outside the Marcellus Shale. Significant gas was produced from the two wells with horizontal fractures in the organic-rich Lower Marcellus Shale, perhaps because twice as much proppant was used as in stages characterized by vertical fracture propagation.

## Geology and geomechanics of the study area

The Middle Devonian Marcellus Shale is one of the largest producing unconventional shale gas plays in North America, spanning parts of four states (New York, Pennsylvania, West Virginia, and Ohio) across the northeastern United States. With proven reserves estimated at more than 70 Tcf of natural gas in Pennsylvania and West Virginia (EIA, 2016), drilling and production have grown rapidly due to the deployment of long-lateral, multistage hydraulic fracturing horizontal wells. Since the commercially successful Renz Unit #1 discovery in the mid-2000s by Range Resources, a number of companies have drilled vertical and horizontal wells across the play to understand the underlying geology of the region and to capitalize on the play's growing gas production (Zagorski et al., 2012).

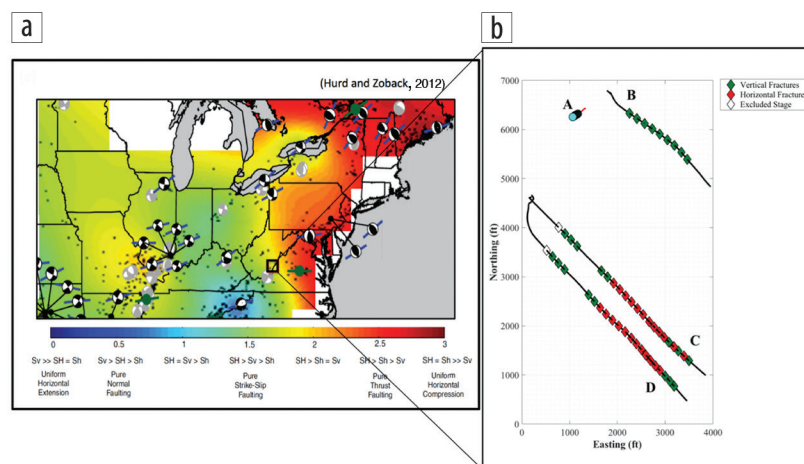


**Figure 1.** (a) The study area shows a strike-slip/reverse faulting stress regime and expected  $S_{Hmax}$  orientation is N50°E (Hurd and Zoback, 2012). (b) Layout of the wells in the study area. Well A is the vertical exploratory well used for geophysical logging and later used to install a monitoring array used to record microseismic events along wells B, C, and D during hydraulic fracturing. As described, stages are color coded to differentiate vertical fractures (green) and horizontal fractures (red). The two stages depicted in white were excluded from our analysis due to an absence of reliable pressure data.

Our study area (Figure 1a, after Hurd and Zoback, 2012) is located in the southeastern part of West Virginia where the stress state is transitional between strike-slip and reverse faulting, and the maximum horizontal principal stress,  $S_{Hmax}$ , is expected to be oriented approximately N50°E. In other words, the least principal stress, which controls the fracturing gradient, is expected to be quite high as  $S_{Hmax} > S_v \sim S_{hmin}$ . As shown in Figure 1b, this study involves one vertical exploration well (A) which was used for geophysical logging, and was followed by the successive drilling of three horizontal production wells (B, C, and D). The horizontal wells targeted the upper part of the Lower Marcellus Shale. All horizontal wells are oriented northwest-southeast (parallel to the  $S_{hmin}$  direction). All of the horizontal wells were hydraulically fractured using the plug-and-perf method with slickwater as the main hydraulic fracturing fluid. Well B was hydraulically fractured from toe to heel in sequence, while wells C and D were zipper fractured. Well A was instrumented with 12 three-component geophones placed immediately above the Lower Marcellus Shale to monitor microseismic activity during hydraulic fracturing in the horizontal wells. A 3D seismic survey was acquired a few years after completion and production from the wells.

The Marcellus Shale is within the lower part of the Hamilton Group, where it is overlain by the Middle Devonian Tully Limestone formation and underlain by the Middle Devonian Onondaga Limestone formation. Geophysical well logs collected from well A (Figure 2) include mineral composition, gamma ray, P- and S-wave sonic velocity, bulk density, and derived Young's modulus. The Marcellus Shale is further subdivided into two shale members, the

<sup>1</sup>Stanford University, Department of Geophysics.

<https://doi.org/10.1190/tle37050356.1>

Upper Marcellus member (sometimes known as the Oatka Creek Shale member) and the Lower Marcellus member (sometimes known as the Union Springs Shale member). The Upper and Lower Marcellus shales are separated by the Cherry Valley Limestone member. The average thickness of the entire Marcellus formation is about 135 ft in the study area. The principal target for stimulation and production, the upper portion of the Lower Marcellus Shale, has an average thickness of less than 20 ft in the study area and is characterized with high organic content (TOC ~6%–8%) and clay content that is slightly lower than that of the Upper Marcellus Shale.

In the left column of Figure 2, the vertical bars indicate the fact that “porpoising” of the horizontal well trajectories resulted in the intersection of several different lithologic units. As discussed at greater length later, wells C and D were mostly in the upper part of the Lower Marcellus Shale (as intended) but also encountered Cherry Valley. Well B was principally in the lower part of the Upper Marcellus Shale and partially in Cherry Valley.

Focusing on the Lower Marcellus Shale, we constructed a quantitative geomechanical model within the study area following the procedures outlined by Zoback (2010) to constrain the orientation and magnitude of the three principal stresses. The orientation of the maximum horizontal compressive stress,  $S_{Hmax}$ , was found to be  $N55^\circ \pm 8E$  from the orientations of drilling-induced tensile fractures observed in a formation microimager (FMI) image log collected in well A (consistent with the regional stress field as shown

in Figure 1a). We integrated the provided bulk density log and determined the magnitude of  $S_V = 58.5$  MPa. The least principal stress ( $S_{hmin}$ ) and pore pressure were provided from a leak-off and extended leak-off test set in the Lower Marcellus Shale in a nearby well and measured to be 56 MPa and 37.3 MPa, respectively. The constrained stress values and selected physical properties of the Lower Marcellus Shale are listed in Table 1. The coefficients of friction and unconfined compressive strength are estimated from laboratory measurements on rocks of similar composition (Zoback et al., 2012; Sone and Zoback, 2013, respectively). As discussed later, the hydraulic fracturing measurements indicate that the least principal stress,  $S_3$ , controlling hydraulic fracture propagation in the Lower Marcellus Shale ranges between  $S_{hmin}$ , which is as low as 56 to 58.5 MPa, the vertical stress. In other words, as expected from the location of the study area, we find that the current stress regime of the Lower Marcellus Shale is strike-slip/reverse faulting, in which the least horizontal principal stress,  $S_{hmin}$ , is of comparable magnitude to the overburden stress,  $S_V$ , such that  $S_{Hmax} > S_V \approx S_{hmin}$ .

### Hydraulic fracture orientation from microseismicity

In Figures 3, 4, and 5, we represent wells C, D, and B in a set of three panels. In each, the top panel shows a profile view of the well’s trajectory, the locations of the perforations associated with each fracture stage, and the distribution of microseismic events associated with each hydraulic fracture stage. Since we

only have a single monitoring array in the study area, we need to remove very small events that are likely due to observational well bias. After comparing the distribution of event sizes with Gutenberg–Richter plots, we set a threshold to exclude all events smaller than moment magnitude  $-2.9$  to ensure catalog completeness across the whole study area. The middle plot shows the well trajectory and perforations for each stage based on the geosteering data collected while drilling and illustrates the geologic formations encountered along the well path. The bottom panel shows the distribution of total proppant volume (blue bars) and the measured instantaneous shut-in pressure (ISIP) value (red points) per stage, whereas the black dashed line is the vertical stress.

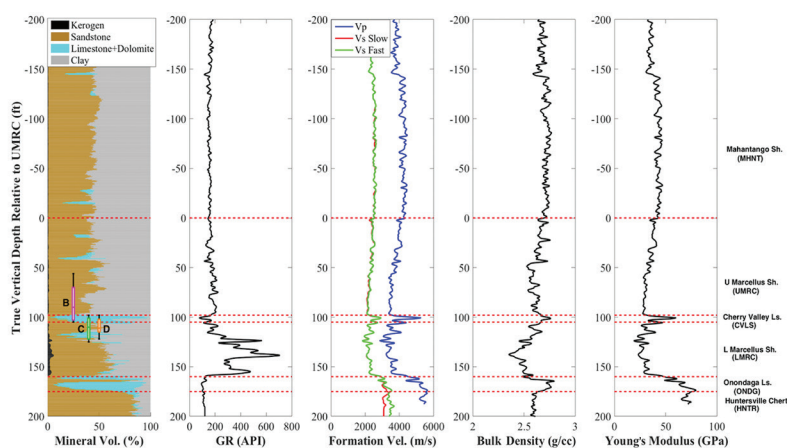


**Figure 2.** Measured well log petrophysics along well A. The far left panel shows mineral volume of clay, sandstone, carbonates, and kerogen while highlighting the horizontal well trajectories intersecting several lithologic units, denoted in whisker and box plots. Box outlines represent the first and third quartiles of the true vertical depth wellhead trajectory relative to the Upper Marcellus Shale. The whisker outlines represent the maxima depth outliers for each well. Formation tops are highlighted in dashed red lines across the subplots.

**Table 1.** Geomechanical model for the Lower Marcellus Shale.

Parameters	Value	Source
$S_V$	58.5 MPa	Integration of density log of well A
$P_p$	37.3 MPa	DFIT data
$S_{hmin}$	>56 MPa	ISIP values from individual hydraulic fracturing stages
Strike of $S_{Hmax}$	$N55^\circ \pm 8E$	FMI log well A
Magnitude of $S_{Hmax}$	102.4 MPa	From observations of drilling-induced tensile fractures in well A
Sliding friction	0.67	Estimated
Unconfined compressive strength	120–170 MPa	Estimated

Starting off with wells C (Figure 3) and D (Figure 4), both wells were zipper fractured using a plug-and-perf setup with slickwater as the fracturing fluid. A total of 21 hydraulic fracturing stages were carried out with a spacing of 140 ft apart along each well. About half of all hydraulic fracturing stages were monitored in each well. Stages 1–10 in well C and stages 1–9 in well D were not monitored for microseismic activity during hydraulic fracturing, presumably because they were so far from the microseismic monitoring array in vertical well A. On the corresponding plots in Figures 3 and 4, we show the center of the perforation locations for those stages as a single black diamond to indicate the formation in which the stimulation took place.

From the top panel of Figure 3 in well C, the microseismic event distribution along stages 11–17 shows the events to be limited within the Lower Marcellus Shale and with a vertical extent of less than 100 ft, while the events from stages 18–21 show microseismic events extending vertically upward over 500 ft and past the Upper Marcellus Shale. The middle panel shows geosteering data of the well trajectory. It is clear that perforation locations for stages 1–17 were placed in the Lower Marcellus Shale, while perforations along stages 18–21 were in the Cherry Valley Limestone. The lower panel of Figure 3 shows the measured ISIPs. We consider the ISIP to be a reliable indicator of the least principal stress, perhaps 2 or 3 MPa (a few hundred psi) higher

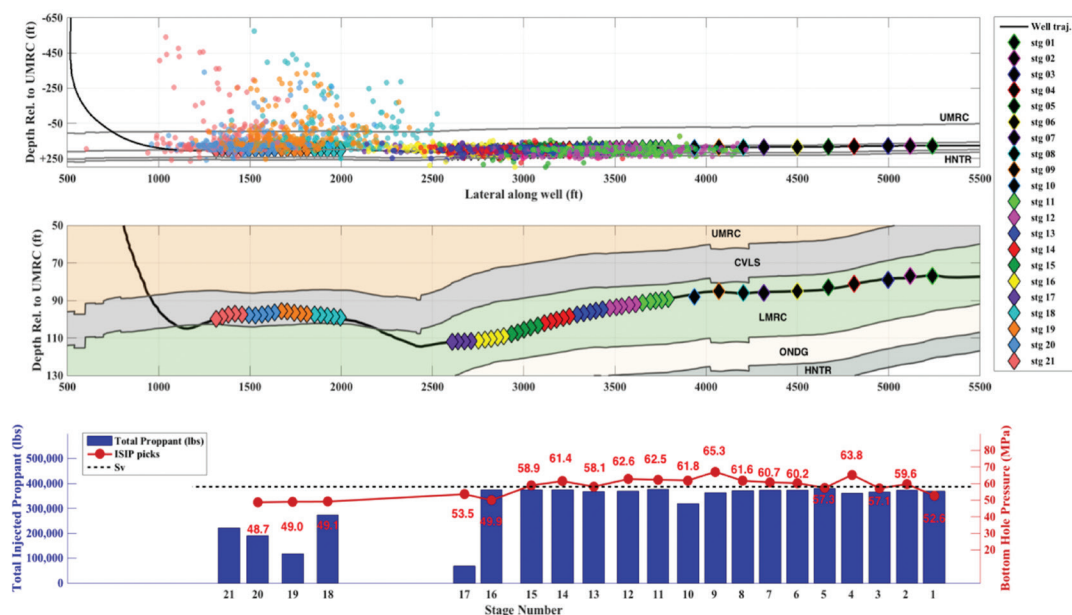


**Figure 3.** The top panel is a profile view of microseismic event distribution along well C across each fracturing stage; only stages 11–21 were monitored for microseismic activity. The middle panel is a vertically exaggerated section highlighting the well trajectory during horizontal drilling. The bottom panel plots total injected proppant volume (bar plot) and measured ISIP (red dots) relative to  $S_v$  (black dashed line) across all stages.

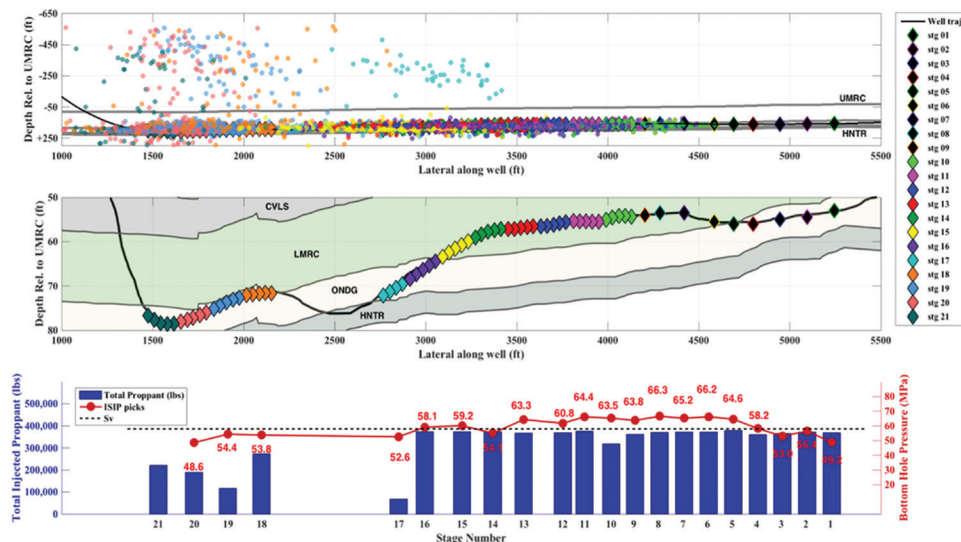


**Figure 4.** The top panel is a profile view of microseismic event distribution along well D across each fracturing stage; only stages 10–21 were monitored for microseismic activity. The middle panel is a vertically exaggerated section highlighting the well trajectory during horizontal drilling. The bottom panel plots total injected proppant volume (bar plot) and measured ISIP (red dots) relative to  $S_v$  (black dashed line) across all stages.



than the pressure at which the hydraulic fracture closes (McClure et al., 2016). Note that for stages 1–16, the ISIPs were approximately equal to (or slightly greater than)  $S_V$ , while stages 17–20 show the measured ISIPs to be less than  $S_V$ , thus corresponding to  $S_{hmin}$ . Note that we excluded stage 21 from analysis because there are no reliable pressure data available for that stage. Because hydraulic fractures propagate in a plane perpendicular to the least principal stress, both the values of the least principal stress for stages 1–16 and the distribution of microseismic events for stages 11–16 indicate horizontal fracture propagation. Recall that no microseismic data were recorded for stages 1–10. All of the fracturing stages for which horizontal hydraulic fracturing seems to have occurred were in the Lower Marcellus Shale.

We show analogous data for well D in Figure 4 and draw similar conclusions as in well C. From the top panel, stages 10–16 show the microseismic events to be limited to within the Lower Marcellus Shale and with a limited vertical extent, while stages 17–21 show microseismic events extending vertically upward over 500 ft and past the Upper Marcellus Shale. Looking closely at the geosteering plot, we can see the stages are split between being placed in the lower part of the Lower Marcellus Shale and the Onondaga Limestone, with stages 1–4 and 16–21 in the Onondaga Limestone and stages 5–15 in the Lower Marcellus Shale. When comparing the ISIPs across the horizontal well, stages 4–16 show measured ISIPs to be approximately equal to or slightly greater than  $S_V$ , while stages 1–3 and 17–20 show measured ISIPs less than  $S_V$ . We thus interpret the least principal stress to be  $S_V$ , resulting in horizontal hydraulic fractures for stages 5–15 in the Lower Marcellus Shale. Coincidentally, we again had to exclude stage 21 from analysis, as there are no reliable pressure readings for that stage as in well C.

In well B (Figure 5), a total of nine hydraulic fracturing stages were carried out with spacing of 180 ft using a conventional plug-and-perf setup with slickwater as the fracturing fluid. The

top panel shows that the microseismic events extend vertically over 350 ft on average for stages 1–7, and over 700 ft for stages 8 and 9 near the heel. The middle panel shows the well trajectory from geosteering data but is absent of interpreted geologic formation horizons; we extend the picked formation tops from well A to well B as a shallowly westward-dipping plane. We show that most of the stage perforations were above the Lower Marcellus Shale based on the extended formation tops, but we are uncertain if they were placed exclusively in the Cherry Valley Limestone or also in the lower part of the Upper Marcellus Shale. Regardless, the lower panel shows the measured ISIP  $< S_V$  for all stages, which we associate with vertical fractures as also observed from microseismicity.

## Discussion

The data noted earlier clearly show that hydraulic fracture propagation for stages in the Lower Marcellus appears to be in a horizontal plane, as the least principal stress is the vertical stress ( $S_V$ ). Hydraulic fractures in the deeper Onondaga, shallower Cherry Valley, and Upper Marcellus propagate in vertical planes, as the least principal stress is  $S_{hmin}$ , which is lower than  $S_V$  in these formations. From a tectonic point of view, this is not particularly surprising because the site is located in a strike-slip/reverse faulting area, where  $S_3 = S_V \sim S_{hmin}$ . Nonetheless, because relatively subtle changes in the magnitude of  $S_3$  have such a profound impact on the orientation of hydraulic fractures, it is important to discuss three key points: (1) what affect does the orientation of hydraulic fractures have on gas production; (2) why is the least principal stress greater in the Lower Marcellus Shale than in both the adjacent deeper and shallower formations; and (3) why, in well D, are there microseismic events above the Lower Marcellus Shale for stages in the Onondaga Limestone, near the heel of the well, as one would have expected vertical fracture propagation to terminate in the Lower Marcellus Shale?

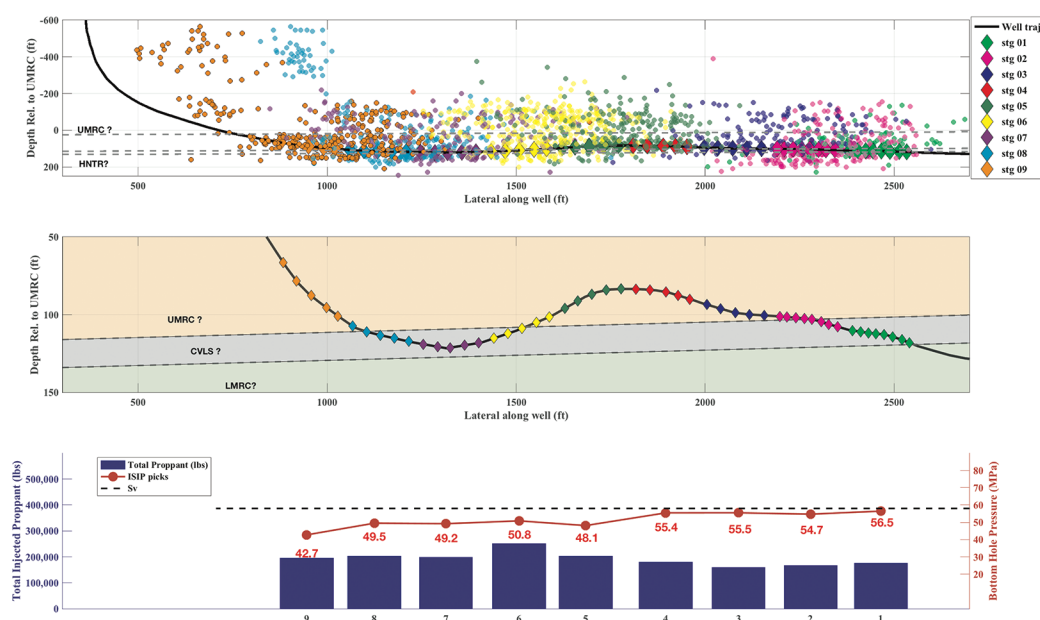


**Figure 5.** The top panel is a profile view of the microseismic event distribution along well B across each fracturing stage. The middle panel is a vertically exaggerated section highlighting the well trajectory during horizontal drilling absent of interpreted geologic formation horizons. We extend the formation tops from well A to well B as a shallowly westward-dipping plane. The bottom panel plots total injected proppant volume (bar plot) and measured ISIP (red dots) relative to  $S_V$  (black dashed line) per fracturing stage.

With respect to well performance, despite being dominated by horizontal hydraulic fracture propagation, daily production reports indicate that wells C and D produced significantly more gas than well B. Because the permeability of unconventional reservoir formations for flow perpendicular to bedding is two to three orders of magnitude lower than for flow parallel to bedding (Al-Ismail et al., 2014), one would not normally consider unconventional wells with horizontal hydraulic fractures to be good producers. One reason wells C and D are such good producers is the large number of stages (17 and 11, respectively) in the organic-rich Lower Marcellus, apparently where the gas is; whereas well B had none. When  $S_{hmin}$  is the least principal stress, vertical hydraulic fracture propagation into the leaner adjacent formations does not appear to contribute significantly to production. It is also important to note that fracturing stages set in the Lower Marcellus Shale with measured ISIPs on the order of  $S_V$  were, in general, treated with twice as much proppant volume as those set in the Cherry Valley Limestone in well C, the Onondaga Limestone in well D (except for stages 1–4), and the Upper Marcellus Shale and the Cherry Valley Limestone in well B. Thus, the combination of focused stimulation in the most gas-rich formation and doing an effective job of propping the fractures seem to have resulted in more productive wells.

The variation in the magnitude of the least principal stress ( $S_3$ ) along the length of the wells seems to correlate with the well trajectory encountering different lithologies. Stages with perforations placed into the clay- and kerogen-rich Lower Marcellus Shale formation yielded  $S_3$  magnitudes on the order of  $S_V$ , while stages with perforations set into the carbonate-rich Cherry Valley Limestone and the Onondaga Limestone formations yielded  $S_3$  magnitudes lower than  $S_V$ , which thus correlate with  $S_{hmin}$ . This increase in the measured ISIP across the Lower Marcellus Shale is likely related to viscoplastic stress relaxation of differential stress, which results in the increase of  $S_{hmin}$  magnitude. Sone and Zoback (2014) demonstrate that compliant geologic formations (i.e., shales high in kerogen and clay content) in unconventional shale gas reservoirs loaded with a constant overburden stress can continually strain over geologic time, causing the stress anisotropy between  $S_V$  and  $S_{hmin}$  within the ductile formation to decrease and become more isotropic over time. This results in a higher fracturing gradient in the Lower Marcellus Shale than for the Onondaga Limestone and Cherry Valley Limestone. Similar cases have been observed in other shale gas plays where viscoplastic stress relaxation in the compliant shale decreases the stress anisotropy between  $S_{hmin}$  and  $S_V$ , for example in the Woodford Shale in Oklahoma (Ma and Zoback, 2017) and in the Permian Basin in west Texas (Xu et al., 2017).

As noted earlier, stages 18–21 near the heel of well D were carried out in the Onondaga Limestone where vertical fracture propagation would be expected. However, one would expect upward vertical fracture propagation to terminate as it reaches the Lower Marcellus Shale, as it should act as a fracture barrier due to its higher fracturing gradient. As we have shown in Figure 4, recorded microseismic events of those stages show events that extend upward around 500 ft, through the Lower Marcellus Shale and up into the Upper Marcellus Shale. Flow

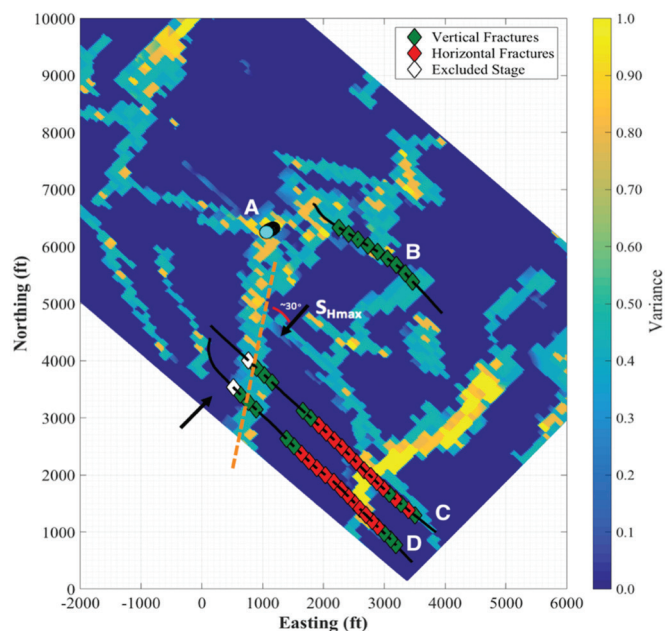


**Figure 6.** A horizon depth slice of the Lower Marcellus Shale showing the extracted 3D variance seismic attribute. In the current stress state of the study area, a strike-slip faulting regime will form a set of conjugate fault planes striking  $30^\circ$  away from the orientation of  $S_{Hmax}$ , where slip could occur on either fault plane. We were able to identify a preexisting natural fault  $30^\circ$  from the orientation of  $S_{Hmax}$  ( $\sim N25^\circ E$ ) and colored in an orange dashed line, which could explain the vertical fracture connection from the Onondaga Limestone across the Lower Marcellus Shale and beyond the Upper Marcellus Shale.

along preexisting faults could potentially explain the vertical fracture connection from the Onondaga Limestone across the Lower Marcellus Shale and beyond the Upper Marcellus Shale, especially if the fault was active in the current stress field (Johri et al., 2014). In the current stress state of the study area, a strike-slip faulting regime will form a set of conjugate fault planes striking  $30^\circ$  away from the orientation of  $S_{Hmax}$ , where slip could occur on either fault plane. With 3D seismic data available in this area, we utilize the variance seismic attribute along the Lower Marcellus Shale formation, using Schlumberger's variance cube volume attribute software, which measures waveform trace dissimilarity, spatially suggesting it be related to faults. Although the signal-to-noise of the 3D seismic volume was not high, we were able to identify a preexisting natural fault  $30^\circ$  from the orientation of  $S_{Hmax}$  ( $\sim N25^\circ E$ ) and colored in an orange dashed line, as shown in Figure 6. This preexisting fault may have slipped during hydraulic fracturing. Regardless, flow along this fault may have allowed pressure to be propagated upward through the Lower Marcellus Shale and beyond the Upper Marcellus Shale, resulting in the recorded microseismic events.

## Conclusion

We presented an integrated analysis of multistage hydraulic fracture stimulation done in three horizontal wells in the Marcellus Shale in southeastern West Virginia where nearly half of all hydraulic fracturing stages examined show evidence of horizontal fracturing, which is indicated by the limited vertical and wide lateral extent of microseismic events, and the measured

values of the least principal stress being equal to or slightly greater than  $S_v$ . We suggest that the high measured ISIPs observed in these stages is due to viscoplastic stress relaxation of the clay- and kerogen-rich Lower Marcellus Shale, which reduces the stress anisotropy between  $S_{hmin}$  and  $S_v$ . Perforation stages set in the Lower Marcellus Shale required the utilization of twice the injected proppant volume compared to stages in which vertical hydraulic fracture propagation occurred. In addition, horizontal fractures induced from perforation stages set in the organic-rich Lower Marcellus Shale contributed significantly to well production without the aid of vertical hydraulic fracture growth. **■**

## Acknowledgments

We would like to thank Bluescape Resources for providing the data set of this study area and for all the personal communications that helped clarify the logistical timelines and production history of the study area. This work was supported by the Stanford Rock Physics and Borehole Geophysics Consortium.

Corresponding author: [alalli@stanford.edu](mailto:alalli@stanford.edu)

## References

- Al Ismail, M., J. S. Reece, S. Hol, and M. D. Zoback, 2014, The effect of CO<sub>2</sub> adsorption on permeability anisotropy in the Eagle Ford Shale: 2<sup>nd</sup> Unconventional Resources Technology Conference, Extended Abstracts, 1119–1127.
- EIA, 2016, U.S. crude oil and natural gas proved reserves, year-end 2015, <https://www.eia.gov/naturalgas/crudeoilreserves/archive/2015/index.php>, accessed 10 April 2018.
- Hurd, O., and M. D. Zoback, 2012, Intraplate earthquakes, regional stress and fault mechanics in the Central and Eastern U.S. and southeastern Canada: *Tectonophysics*, **581**, 182–192, <https://doi.org/10.1016/j.tecto.2012.04.002>.
- Johri, M., M. D. Zoback, and P. Hennings, 2014, A scaling law to characterize fault-damage zones at reservoir depths: *AAPG Bulletin*, **98**, no. 10, 2057–2079, <https://doi.org/10.1306/05061413173>.
- Ma, X., and M. D. Zoback, 2017, Lithology-controlled stress variations and pad-scale faults: A case study of hydraulic fracturing in the Woodford Shale, Oklahoma: *Geophysics*, **82**, no. 6, ID35–ID44, <https://doi.org/10.1190/geo2017-0044.1>.
- McClure, M. W., H. Jung, D. D. Cramer, and M. M. Sharma, 2016, The fracture-compliance method for picking closure pressure from diagnostic fracture-injection tests: *SPE Journal*, **21**, no. 4, 1321–1339, <https://doi.org/10.2118/179725-PA>.
- Sone, H., and M. D. Zoback, 2013, Mechanical properties of shale-gas reservoir rocks — Part 2: Ductile creep, brittle strength, and their relation to the elastic modulus: *Geophysics*, **78**, no. 5, D393–D402, <https://doi.org/10.1190/geo2013-0051.1>.
- Sone, H., and M. D. Zoback, 2014, Time-dependent deformation of shale gas reservoir rocks and its long-term effect on the in situ state of stress: *International Journal of Rock Mechanics and Mining Sciences*, **69**, 120–132, <https://doi.org/10.1016/j.ijrmms.2014.04.002>.
- Xu, S., F. Rassouli, and M. Zoback, 2017, Utilizing a viscoplastic stress relaxation model to study vertical hydraulic fracture propagation in Permian Basin: 5<sup>th</sup> Unconventional Resources Technology Conference, Extended Abstracts, 787–791.
- Zagorski, W. A., R. W. Gregory, and D. C. Bowman, 2012, The Appalachian Basin Marcellus gas play: Its history of development, geologic controls on production, and future potential as a world-class reservoir, *in* J. A. Breyer, ed., *Shale reservoirs: Giant resources for the 21<sup>st</sup> century*: AAPG Memoir, **97**, 172–200.
- Zoback, M. D., 2010, *Reservoir geomechanics*: Cambridge University Press.
- Zoback, M. D., A. Kohli, I. Das, and M. W. McClure, 2012, The importance of slow slip on faults during hydraulic fracturing stimulation of shale gas reservoirs: Americas Unconventional Resources Conference, Society of Petroleum Engineers.